InGaAs/InGaAsP MQW Electroabsorption Modulator Integrated with a DFB Laser Fabricated by Band-Gap Energy Control Selective Area MOCVD

Masahiro Aoki, Makoto Suzuki, Hirohisa Sano, Toshihiro Kawano, Tatemi Ido, Tsuyoshi Taniwatari, Kazuhisa Uomi, and Atsushi Takai

Abstract—**Fabrication and basic characteristics of a new structure InGaAs/InGaAsP (MQW) electroabsorption modulator integrated with a distributed feedback (DFB) laser are presented. First, a fundamental study was performed on the applicability of the InGaAs/InGaAsP MQW structure to an electroabsorption-type modulator. We have experimentally demonstrated both the efficient attenuation, the small hole pile-up and small chirp characteristics of a discrete modulator based on this MQW structure. We also made a study of the controllability of in-plane band-gap energy by the use of selective area metal-organic chemical vapor deposition aimed at one-step growth integration of modulators and lasers. We demonstrated a sufficient range for controllable quantum energy level and high quality of the selectively grown MQW layers.**

By using this technique, the modulator was monolithically integrated with a same-material MQW DFB laser. Using a low-capacitance semi-insulating buried-hetero structure, we achieved over 14-GHz modulation under high-light-output operations up to +10 dBm. Modulation at 10 Gb/s with a modulation voltage swing of only 1 V_{pp} demonstrates the potential value of this InGaAs/InGaAsP MQW system for laser-integrated electroabsorption modulators for 1.55 μm lightwave communications.

I. Introduction

RECENTLY, due to the development of erbium-doped fiber amplifiers, a dramatic extension has been achieved in loss-limited distance for multigigabit optical fiber communication systems [1]. In such chirp-limited transmission, a low-chirp transmitter in the 1.55 μm wavelength range is an essential component. Therefore, intensive efforts have been made to achieve external optical modulators to overcome the large-wavelength chirp observed in conventional direct modulation of laser diodes. Among various types of optical modulators, multiple-quantum-well (MQW) optical modulators consisting of III/V compound semiconductors have become promising candidates [2]–[10]. These MQW modulators enable high-speed, low-chirp, and highly efficient modulations based on large field-induced variations in absorption coefficients or refractive indices by the quantum-confinement Stark effect (QCSE).

Among the various types of QCSE modulators, the electroabsorption (EA) type has a large potential for practical use because of simplicity of its device physics as well as its high structural feasibility for monolithic integration with lasers [11]–[20]. Concerning materials, most of the 1.55-μm EA modulators so far reported have used MQW structures with InGaAs wells (or related quaternary wells such as InGaAlAs or InGaAsP) and barriers made out of InAlAs [3]–[5] or InP [6], [7]. We note that, in these MQW modulators, the barrier materials which give rather large well/barrier band discontinuities were chosen to achieve sufficient quantum confinement for enhancing the QCSE. Conversely, an InGaAs(P)/InGaAsP MQW system that has given satisfactory results in long-wavelength lasers is an alternative candidate for EA-type modulators [8], [16]–[20]. The band offsets of the InGaAs(P)/InGaAsP MQW system are relatively small; that is the quantum well is rather shallow compared with the former MQW systems. However, we can expect enhanced sweep out of photogenerated carriers outside quantum wells. This is another important feature for achieving better modulator performance under higher light power operation [8], [21]–[24]. This will be a problem when a light-source laser is integrated monolithically. One of our aims herein is to clarify the applicability of the InGaAs/InGaAsP MQW structure to an EA-type modulator for the purpose of modulator/laser integration from the same-material MQW structure.

One major difficulty in fabricating photonic integrated devices has been to reproduce good optical waveguide coupling between the functional elements. Although the modulators and lasers share almost the same fabrication technology, it is still difficult to create a smooth and high-quality crystal in the interface between the functions by using conventional integration techniques in which each functional element is grown separately using selective etching followed by regrowths. In addition, both modulators and lasers have been improved dramatically by using the quantum size effect in MQW structures, but it has been quite difficult to integrate the different MQW structures.

Selective area growth (SAG) using metal-organic chemical vapor deposition (MOCVD) has attracted much attention recently because it offers a new degree of freedom in designing epitaxial parameters [25]–[31]. The

Manuscript received November 1, 1992; revised February 4, 1993.

The authors are with the Central Research Laboratory, Hitachi Ltd., Tokyo, Japan.

IEEE Log Number 9209159.

technique not only restricts crystal growth into photolithographically defined windows of dielectric films formed on the substrate, it also adjusts the grown layer thicknesses and material compositions—and thus the band-gap energy (*Eg*)—independently in different areas on the same substrate during simultaneous epitaxy. The resultant variations in *Eg* and thickness of bulk III–V compounds, however, have not been large because except for binary bulks they are limited by the associated deviation of the lattice constant of the device epitaxial layer from that of the substrate [25], [26].

Recently, a new photonic device integration scheme has been proposed using the SAG of MQW structures [16]–[20], [28], [29]. This technique, which we call "in-plane band-gap energy control" is based on the SAG-induced growth rate enhancement or compositional changes in the material of the quantum-well layer. We can modify the equivalent *Eg* (i.e., the quantum energy level) of the selectively grown MQW layer simply by changing the selective mask dimension along the optical axis. Thus, this integration method has the following advantages:

1) The local *Eg* of simultaneously grown structures can be controlled easily by designing the photolithographically defined selective masks.
2) A number of MQW structures with different *Eg* can be integrated simultaneously, which will be essential for large-scale integration.
3) The optical coupling between functional devices can be made almost 100% automatically because all the integrated elements consist of one continuous MQW crystal with a taperlike coupling portion between them.
4) We can obtain high-quality crystals free from the associated deviation of the lattice constant since the thickness of each selectively grown MQW layer can be designed below the critical thickness.

In the next section, first, we investigate the basic properties of a discrete EA modulator with an InGaAs/InGaAsP MQW structure to examine the compatibility of this material for the modulators and lasers. The results are then compared directly with those of InGaAs/InAlAs EA modulators [5]. As a result, we demonstrated, for the first time, that the InGaAs/InGaAsP MQW modulators can be compared with InGaAs/InAlAs MQW modulators from the viewpoints of modulation efficiency, modulation bandwidth related to the hole pile-up and the magnitude of phase chirp expressed by the linewidth broadening factor.

In Section III, we describe the controllability of the in-plane *Eg* and quality of the SAG-MQW crystals. In Section IV, we show the fabrication and device performance of an InGaAs/InGaAsP MQW EA modulator monolithically integrated with the same-material MQW DFB laser by using our new integration technique. We show how the precise adjustment of the local *Eg* and an inherently perfect optical coupling lead to excellent properties of the integrated device.

II. Discrete EA Modulator Based on an InGaAs/InGaAsP MQW Structure

A. Device Structure and Design

First, a fundamental study was performed on the electroabsorption, high-speed, and phase-chirp characteristics of a discrete InGaAs/InGaAsP MQW EA modulator. Fig. 1 shows the schematic structure of the fabricated MQW EA modulator. The device, based on the InGaAs/InGaAsP MQW, a separate confined heterostructure (SCH) and a planar semi-insulating buried-hetero (BH) structure, was grown entirely by low-pressure MOCVD. The waveguide was aligned along the [011] direction. Both cleaved facets were coated with SiN_x antireflective ($\sim 1\%$) films. The MQW absorption layer consists of five InGaAs wells (5 nm thick) separated by InGaAsP barriers (8 nm thick). The photoluminescence (PL) peak waveguide (λ_{PL}) of the MQW layer was set to around 1.49 μm. InGaAsP with a band-gap wavelength (λ_g) of 1.15 μm was chosen for the barrier layers. This makes the valence band discontinuity of InGaAs/InGaAsP MQW's ($\Delta E_v \sim$ 0.2 eV) almost the same as that of InGaAs/InAlAs systems. We note that, using the latter system, Wakita *et al.* have demonstrated an intrinsic modulation bandwidth over 40 GHz [3]. This means that this InGaAs/InAlAs MQW system is almost free from hole pile-up, which results from rather shallow valence band wells for holes with large effective mass. Conversely, in an InGaAs/InP MQW system whose ΔE_v has a rather large value of 0.38 eV, a decrease in bandwidth at high optical intensity has been observed clearly to be caused by the hole pile-up [6]. To overcome this degradation, Wood *et al.* demonstrated experimentally the increased EA saturation intensities in InGaAs MQW's by using InGaAlAs (λ_g = 1.17 μm) as a barrier material [23]. They also predicted better results by the use of thin InGaAsP barriers. Thus, the preceding discussion implies a small hole pile-up in the InGaAs/InGaAsP MQW EA modulator.

B. Attenuation Property

Next, attenuation characteristics of the fabricated MQW EA modulator were measured. Transverse electric (TE) polarized light from a wavelength-tunable semiconductor laser (Santec TSL-80) or a 1.554 μm DFB laser was used for the input. Tapered microlens single-mode fibers were used for focusing on the modulator waveguide. Fig. 2 shows typical attenuation characteristics of a 190-μm-long device for 1.55- and 1.57-μm wavelength. The intensity of incident light was -3 dBm for both cases. At 1.55 μm, we obtained on/off ratios of 8 dB and 16 dB for applied reverse voltage of 1 V and 2 V, respectively. However, the absorption seems to saturate when the bias increases further, as can be seen in the figure. To understand this saturation, dependence of optical absorption on the incident optical intensity was evaluated. Fig. 3 shows the measured photogenerated current I_{ph} as a function of intensity of incident light from the DFB laser (λ = 1.554 μm). To enhance the accumulation of photogenerated carriers, no bias was applied to the modulator. We found no

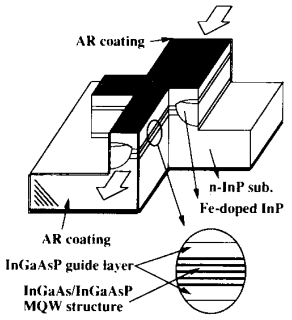

Fig. 1. Structure of InGaAs/InGaAsP MQW EA modulator.

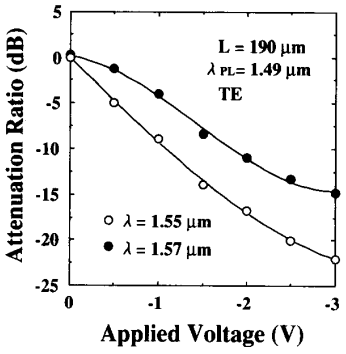

Fig. 2. Attenuation characteristics.

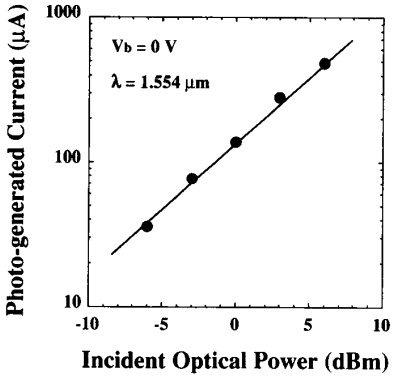

Fig. 3. Photogenerated current as a function of incident power.

saturation of I_{ph} as the optical intensity increased to +6 dBm. This means that the saturated on/off ratio observed in Fig. 2 is not caused by carrier pile-up. This might be explained by the saturated field-induced change in absorption coefficient due to absorption edge broadening at higher electric fields. The explanation seems reasonable by considering the small-conduction-band discontinuity of the present InGaAs/InGaAsP MQW ($\Delta E_c \sim 0.13$ eV) and, accordingly, the electron wave function becomes leaky under higher field intensities.

C. High-Speed Properties

Next, small-signal frequency response was measured using a component analyzer (HP8703A). Before the measurement, a 50-Ω load resistor was mounted near the modulator chips to eliminate microwave signal reflection. The intensity of the electrical RF signal and dc reverse bias applied to the modulator were 5 dBm and 1 V, respectively. Fig. 4 illustrates the measured electrical response at several values of incident optical power. The 3-dB down bandwidth was about 14 GHz, which roughly corresponds to a parasitic capacitance of 0.38 pF measured by the *C-V* method at 1 MHz. A more important point is that the bandwidths are insensitive to the incident optical power up to +6 dBm, and that the bandwidth is limited only by the parasitics. The results imply small hole pile-up in our InGaAs/InGaAsP MQW EA modulator and its capability of much higher speed modulation by the reduction of parasitic capacitance.

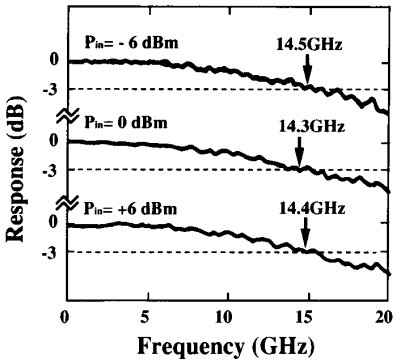

Fig. 4. Frequency response at various incident optical powers.

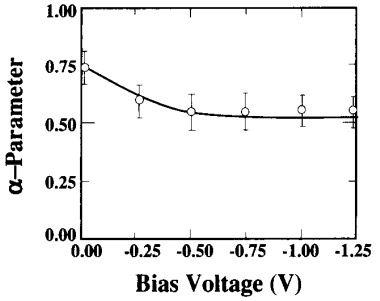

Fig. 5. Measured α parameter as a function of bias voltage.

Next, the linewidth broadening factor (α parameter), which determines the amount of phase chirp, is examined. The α parameter was estimated by measuring the relationship between the relative strength of sideband to carrier and the intensity modulation index when the modulator is modulated sinusoidally at 900 MHz [32]. Fig. 5 plots the measured α values as a function of applied bias voltage. The α values were found to range from 0.5 to 0.75, depending on the applied bias levels. These values were comparable or even smaller than those reported for the InGaAs/InAlAs MQW EA modulators.

D. Comparison of InGaAs/InGaAsP and InGaAs/InAlAs MQW EA Modulators

Table I summarizes the preceding modulator characteristics for the present InGaAs/InGaAsP MQW EA mod-

TABLE I
COMPARISON OF InGaAs/InGaAsP AND InGaAs/InAlAs [5] MQW EA MODULATOR

Well/Barrier Materials	Well Thickness	Optical Confinement Factor in Well Layer	Modulation Efficiency (λ = 1.55 μm, 0 to 2 V)	Maximum Allowable Power	α-parameter
InGaAs/InGaAsP	5 nm	5.2%	8.4 dB/100 μm	more than 6 dBm	0.5 ~ 0.75
InGaAs/InAlAs [5]	7 nm	7.1%	14.0 dB/100 μm	more than 8 dBm	0.5 ~ 1.0

ulator along with those for the InGaAs/InAlAs MQW EA modulators [5]. Here, both kinds of modulator have the five InGaAs wells and almost the same quantum energy level (λ_{PL} ~ 1.49 μm). We notice that the modulation efficiency of the InGaAs/InAlAs MQW modulator is about 1.6 times larger than that of the InGaAs/InGaAsP system. This results simply from the thinner InGaAs well thickness in the case of the InGaAsP barrier, that is, smaller QCSE and the smaller optical confinement factor in the well layer. We can solve this, for example, by the use of an InGaAsP quaternary [8] or a small amount of tensile strain in the well layer to widen the well. Conversely, it is clear from Table I that the InGaAs/InGaAsP MQW modulators can be compared with InGaAs/InAlAs MQW modulators from the viewpoints of modulation bandwidth with respect to the hole pile-up and the magnitude of phase chirp determined by the α parameter. These results indicate that the InGaAs/InGaAsP MQW material can be used in practice for an EA-type modulator for 1.55-μm lightwave communications.

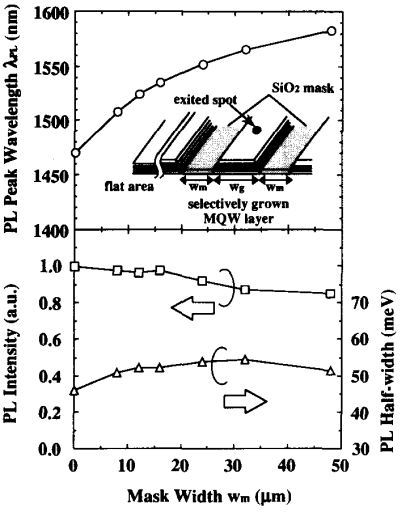

Fig. 6. Controllability of the in-plane band-gap energy and crystal quality of selectively grown MQW layers.

III. IN-PLANE BAND-GAP ENERGY CONTROL BY SAG-MOCVD

In this section, the fundamentals of the in-plane band-gap energy control technique are described focused mainly on the *Eg* controllability and quality of the SAG crystal. We used thermal chemical vapor deposited (T-CVD) silicon dioxide (SiO_2) for the selective mask material, because this material is physically and chemically more stable than dielectrics such as silicon nitride (SiN_x) or amorphous silicon (a-Si) and because the resultant growth selectivity is also better. Parallel stripes of 0.2-μm-thick SiO_2 film were formed on a (100) InP substrate along the [011] direction (see inset in Fig. 6) using the T-CVD and standard photolithography followed by wet chemical etching by buffered HF solution. The width of the growth region between the mask stripes (w_g) and width of the mask stripe (w_m) were set to ~ 10–60 μm. Then a ten-pair InGaAs/InGaAsP MQW structure was grown both on the patterned and flat substrates by low-pressure MOCVD (40 torr, 600°C). The MQW consisted of 5-nm-thick InGaAs wells separated by 10 nm thick InGaAsP (λ_g = 1.15 μm) barriers. Growth conditions were chosen so that all the epitaxial layers other than the InGaAs well were lattice-matched to an unmasked InP substrate. To compensate for the increased indium content in the selectively grown layers, the lattice constant of the InGaAs well in the unmasked section was set 0.3% shorter than that of the InP substrate ($\Delta a/a = -0.3\%$). This is very effective for obtaining high-quality selectively grown MQW layers, which will be detailed elsewhere.

The selectively grown layers were characterized by measuring their microscopic photoluminescence ["μ" developed by Atago Bussan Ltd.] at room temperature. An argon laser (wavelength = 514.5 nm) was used for the excitation source. The incident probe power density and spatial resolution defined by the *x-y* stage were typically 50 W/cm^2 and 0.05 μm, respectively. The excitation light was collimated into a spot 1 μm in diameter on the top surface of the samples. The PL emission was detected through two sets of 100 μm wide slits arranged at right angles to eliminate the stray light caused by the carrier diffusion around the excited spot. Fig. 6 shows the changes in the PL peak wavelengths (λ_{PL}) measured at the center of the growth regions, when the mask width (w_m) was changed from 0 (flat area) to 48μm while the width of the growth region (w_g = 16 μm) was kept constant. The λ_{PL} was controlled from 1.47 to 1.58 μm, over a 110-nm-wavelength window around 1.5 μm, which is large enough to achieve modulator/laser integration. This wide range of controllable λ_{PL} is clearly attributed to the change in quantum energy levels associated with the large intentional difference in InGaAs well thicknesses and also with the difference in well layer compositions caused by adjustments in the supply of group III atoms through the masks [25], [26]. Fig. 6 also shows the corresponding peak intensities and the half-widths of this PL. The results

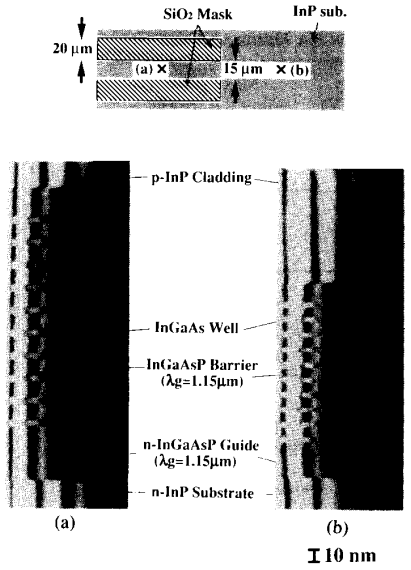

Fig. 7. CAT-TEM images of (a) SAG-MQW layer compared with (b) normally grown MQW layer.

indicate that crystal quality of selectively grown layers is almost as good as that of normally grown layers on the flat substrate.

Next, we directly observed the selectively grown MQW structure by transmission electron microscope using the composition analysis by thickness fringe method (CAT-TEM) [33]. Fig. 7 shows a typical CAT-TEM image for the selectively grown MQW layer (w_m = 20 μm, w_g = 15 μm) compared with that for a simultaneously grown reference layer on the adjacent flat region (see inset in Fig. 7). We clearly observed an SAG-caused enhancement in layer thicknesses and a high uniformity in the layer thicknesses and compositions in the growth direction (expressed by the homogeneous equal thickness fringes in the vertical direction). The enhanced growth rate ratios are about 1.3 and 1.6 for InGaAs wells and InGaAsP barriers, respectively, and these values are consistent with those for bulk layers previously measured. Moreover, a steep well/barrier heterointerface can be seen for this selectively grown MQW, just the same as for the reference layer. These results ensure the high quality of SAG layers.

This new integration can have a wide variety of applications, such as modulator integrated DFB lasers [16]–[20], butt-jointless DBR lasers [34] or any type of integrated active/passive waveguides [35] toward more functional optical devices.

IV. An InGaAs/InGaAsP MQW EA Modulator Integrated with a DFB Laser

A. Device Structure and Fabrication

This section describes the device structure, fabrication, and performance of an InGaAs/InGaAsP MQW EA modulator integrated with a DFB laser on the basis of Sections II and III.

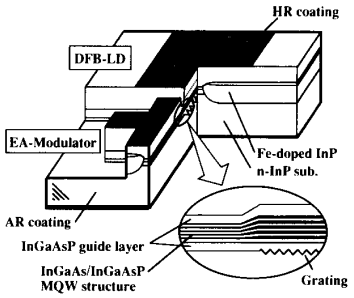

Fig. 8. Structure of the DFB-laser-integrated EA modulator based on InGaAs/InGaAsP MQW structure.

Fig. 8 illustrates the schematic structure of the device. The modulator absorption layer and laser active layer consist of one continuous SCH-InGaAs/InGaAsP MQW structure with slightly different thicknesses and composition. The bandgap energies of the MQW waveguides for the modulator and laser were controlled by using SAG, as described in Section III. The fabrication process is illustrated in Fig. 9. Initially, a conventional first-order grating was partially etched in the laser section on a (100) n-InP substrate. Then, a 0.15-μm-thick n-InGaAsP (λ_g = 1.15 μm) lower optical guide layer and 10-nm-thick n-InP cap layer were grown entirely on the partially corrugated substrate. Next, an SAG mask made of 0.2-μm-thick SiO_2 was formed [Fig. 9(a)]. An actual mask pattern is shown in the upper part of Fig. 10. It consists of a pair of 15-μm-wide SiO_2 stripes with 10-μm separation formed only in the laser section. Note that these dimensions were chosen to be much smaller than the length of vapor phase diffusion for the grown species (L_{diff} = 30–50 μm) in our MOCVD conditions; this is important to obtain highly uniform SAG layers between the selective masks [36]. On this patterned wafer, successive MOCVD-SAG was performed to grow an InGaAs/InGaAsP MQW structure (five wells, λ_{PL} = 1.49 μm on the modulator section), an InGaAsP upper optical guide layer (λ_g = 1.15 μm), a p-InP cladding layer, and an InGaAsP cap layer [Fig. 9(b)]. The growth conditions for the well layer were adjusted to obtain a 0.3% tensile grain in the modulator section in the unmasked area. This was to obtain wider wells in the modulator section for enhancing QCSE and also for better quality of SAG crystal in the laser section, as mentioned in Section III. Fig. 10 plots the λ_{PL} of the prototype MQW layer measured in 10-μm steps along the optical axis by using the microscopic PL. The flat distribution of PL peak intensity shown in Fig. 10 indicates the light quality of the SAG crystal. Moreover, λ_{PL} was adjusted precisely to 1.49 and 1.565 μm for the two sections by the designed SAG mask dimensions. Furthermore, the length of the λ_{PL} transition region between the sections was found to be less than 50 μm, which roughly corresponds to the L_{diff} values. We notice that this band-gap transition region produces extra loss which guided light suffers as it propagates through this loss-varying region, and this optical loss may lead to the degradation of the effective optical coupling. By a simple calculation assum-

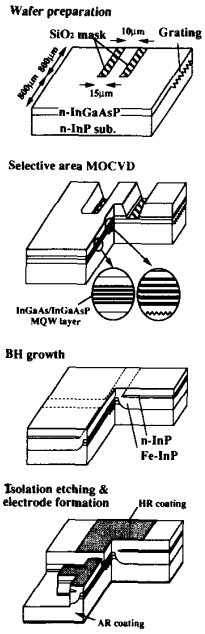

Fig. 9. Fabrication process.

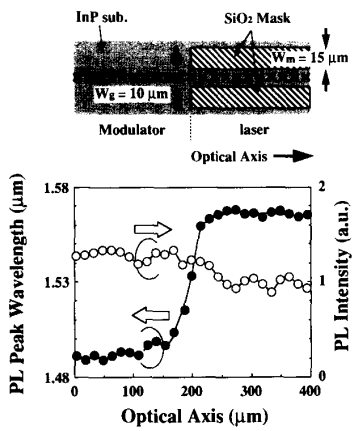

Fig. 10. λ_{PL} measured along the optical axis.

ing a linearly graded loss distribution, total optical loss in the 50-μm-long band-gap transition is estimated to be less than 0.5 dB for a 1.55 μm wavelength.

Following the SAG, the wafer was processed into a planar BH structure with a 3.5-μm-thick semi-insulating (SI) layer doped by 1.5×10^{17} cm^{-3} Fe [Fig. 9(c)]. To reduce the parasitic capacitance further, a 10-μm-wide narrow mesa structure was included in the modulator part. A 0.3 μm thick n-InP hole blocking layer was introduced between the SI and p-InP cladding layers. For the electrical isolation, the n-InP layer was etched partially between the modulator and laser. The resultant isolation resistance was typically 10 kΩ. Fig. 11 shows the scanning electron microscope (SEM) photographs of the cross section for

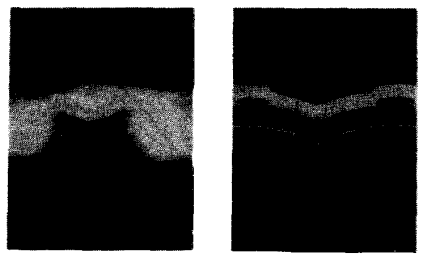

Fig. 11. SEM views of cross section of the device: (a) modulator; (b) laser.

the modulator and laser. The modulator output facet was coated with an antireflective (0.2%) film to avoid the optical feedback of laser light from the modulator facet. The laser rear facet was closed with a highly reflective film (90%) to enlarge the output efficiency of the lasing light [Fig. 9(d)].

B. Static Properties

The device had low threshold currents (5.4 mA minimum), high quantum efficiencies (0.19 W/A maximum), and high output power (25 mW maximum). Fig. 12 shows typical *I–L* curves of the 800-μm-long device (laser 500 μm, modulator 260 μm, separation 40μm). The threshold current and the slope efficiency without modulation bias were 9.0 mA and 0.18 W/A, respectively. The kink-free maximum output power was 14 mW in this case. These lasing properties, comparable even with those of discrete lasers, reflect the high SAG crystal quality, the efficient waveguide coupling between the devices, and sufficient current blocking by the thick Fe-doped layer. Clear attenuation was observed when reverse voltages were applied to the modulator. We found that the residual light output at higher applied voltage was very small, which resulted in an on/off ratio of more than 20 : 1 (extinction ratio of 13 dB) when the bias was changed from 0 to -2 V. This means that the light scattering at the modulator/laser coupling portion is reduced effectively by the inherently perfect optical coupling of our integration scheme. Fig. 13 shows the attenuation characteristics of this device measured from the output light coupled into the tapered microlens fiber with different laser driving currents. Note that for any of the laser driving conditions, the optical power (P_{in}) directly injected into the modualtor exceeds +3 dBm. We found that attenuation curves were similar to those of the discrete modulator shown in Fig. 2, and that their dependence on the laser driving currents, that is, the dependence on the optical intensity, was sufficiently small.

C. High-Speed Properties

The small-signal frequency response was measured for the device with a 200 μm long modulator using a dc bias of -1.5 V and a 5 dBm RF signal. The measured 3 dB frequency bandwidth shown in Fig. 14 was over 14 GHz,

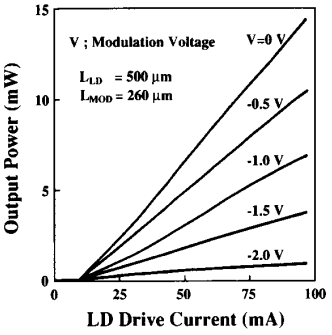

Fig. 12. Typical I–L curves.

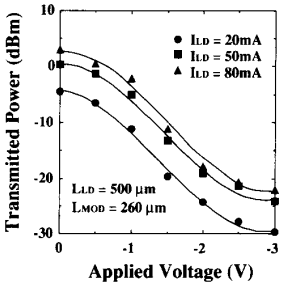

Fig. 13. Attenuation characteristics.

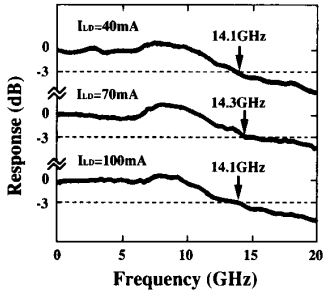

Fig. 14. Frequency response at various laser driving currents.

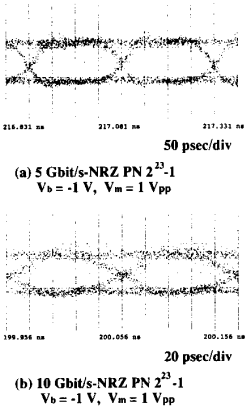

Fig. 15. Eye pattern for (a) 5 and (b) 10 Gb/s NRZ modulation.

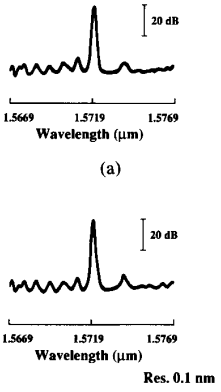

Fig. 16. Lasing spectrum under (a) 10-Gb/s NRZ modulation and (b) that of CW light.

which is almost the same value as that of the 190 μm long discrete modulator shown in Fig. 4. Moreover, we observed no significant change in the response when the laser driving current was increased from 40 (P_{in} = 4 dBm) to 100 mA (P_{in} = 12 dBm). Fig. 15 shows the eye pattern for NRZ $2^{23} - 1$ pseudorandom modulation at a signal rate of 5 and 10 Gb/s. The laser driving current was set so that the peak output power guided through the modulator was +7 dBm at the "on" level. A clear eye opening was attained at this high-power operation with a modulation voltage swing of only 1 V_{pp} and a bias voltage of −1 V. These experimental results provide direct proof of the small carrier pile-up and the high EA-modulation efficiency of this InGaAs/InGaAsP MQW system. Fig. 16 shows the lasing spectrum of this 10-Gb/s modulation along with the lasing spectrum of CW light. Stable single longitudinal mode (SLM) SLM operation was observed with a side-mode suppression ratio greater than 35 dB. The change in spectrum width due to the modulation was less than the measurement resolution of 0.1 nm.

V. Conclusion

We have presented the basic characteristics of an InGaAs/InGaAsP multiple-quantum-well (MQW) electroabsorption modulator, focusing on the modulation efficiency, high-speed performance restricted by the carrier pile-up, and the magnitude of phase chirp. We have experimentally demonstrated both the efficient attenuation at low field and the small hole pile-up of this modulator. Moreover, the linewidth broadening factor was found to be as small as 0.5–0.6. These results, which we have demonstrated for the first time, are comparable with InGaAs/InAlAs MQW modulators.

We also made a fundamental study of the controllability of in-plane band-gap energy and crystal quality of selectively grown InGaAs/InGaAsP MQW structures aimed at one-step growth integration of modulators and lasers. We demonstrated a sufficient range for controllable band-gap energy and high quality of the selectively grown MQW layers.

The InGaAs/InGaAsP MQW electroabsorption modulator was monolithically integrated with the same-material MQW direct feedback laser by using the in-plane band-gap energy control technique. Using a low-capacitance semi-insulating buried-hetero structure, we achieved over 14 GHz modulation bandwidth, which is not influenced by the laser driving conditions. Modulation at 10 Gb/s with a modulation voltage swing of only 1 V_{pp} demonstrates the potential value of this InGaAs/InGaAsP MQW system for electroabsorption modulation in 1.55-μm lightwave communications.

One possible disadvantage of this integration may lie in the difficulty of optimizing the MQW structure for each integrated element, since the MQW material and well number is always the same for all functions integrated this way. The optimal MQW structures are, however, similar for injection lasers and electroabsorption modulators because their fundamental physical mechanism, carrier injection/extraction, and light emission/light absorption, are also very similar.

ACKNOWLEDGMENT

The authors would like to thank N. Chinone, K. Ishida, Y. Ono, and S. Sasaki for their continuous encouragement throughout this work. They also acknowledge the valuable experimental contributions made by K. Saito, T. Kaneko, M. Haneda, H. Tsushima, H. Matsuda, T. Tsuchiya, and M. Takahashi.

REFERENCES

[1] Special Issue on Optical Amplifiers, *J. Lightwave Technol.*, vol. 9, pp. 145-296, Feb. 1991.

[2] T. H. Wood, "Multiple quantum well waveguide modulators," *J. Lightwave Technol.*, vol. 6, pp. 743-757, 1988.

[3] K. Wakita, I. Kotaka, O. Mitomi, H. Asai, Y. Kawamura, and M. Naganuma, "High-speed InGaAs/InAlAs multiple quantum well optical modulators with bandwidths in excess of 40 GHz at 1.55 μm," in *Proc. Conf. Lasers Electro-Opt. CLEO '90*, Anaheim, CA, Paper CtuC6, 1990.

[4] K. Wakita, I. Kotaka, O. Mitomi, H. Asai, O. Mikami, Y. Kawamura, and M. Naganuma, "High-speed InGaAlAs/InAlAs multiple quantum well optical modulators," *J. Lightwave Technol.*, vol. 8, pp. 1027-1031, 1990.

[5] H. Sano, H. Inoue, H. Nakamura, K. Ishida, and J. M. Glinski, "Low loss single-mode InGaAs/InAlAs multiquantum well electroabsorption modulator," in *Tech. Dig. OFC '90*, San Francisco, CA, Paper WM15, 1990.

[6] U. Koren, B. I. Miller, T. L. Koch, G. Eisenstein, R. S. Tucker, I. Bar-Joseph,and D. S. Chemla, "Low-loss InGaAs/InP MQW optical electroabsorption waveguide modulator," *Appl. Phys. Lett.*, vol. 51, pp. 1132-1134, 1987.

[7] F. Devaux, E. Bigan, B. Rose, M. Mckee, F. Huet, and M. Carre, "High-speed, InGaAsP/InP multiple quantum 1.55 μm singlemode modulator," *Electron. Lett.*, vol. 27, pp. 1926-1927, 1991.

[8] F. Devaux, E. Bigan, A. Ougazzaden, B. Pierre, F. Huet, M. Carre, and A. Carenco, "InGaAsP/InGaAsP multiple quantum well modulator with improved saturation intensity and bandwidth over 20 GHz," *IEEE Photon. Technol. Lett.*, vol. 4, pp. 720-722, 1992.

[9] H. Sano, H. Inoue, S. Tsuji, and K. Ishida, "InGaAs/InAlAs MQW Mach-Zehnder optical modulator for 10-Gbit/s long-haul transmission systems," in *Tech. Dig. OFC '92*, San Jose, CA, Paper ThG4, 1992.

[10] J. E. Zucker, K. L. Jones, B. I. Miller, M. G. Young, U. Koren, B. Tell, and K. Brownn-Goebeler, "Interferometric quantum well modulators with gain," *J. Lightwave Technol.*, vol. 6, pp. 924-932, 1992.

[11] Y. Kawamura, K. Wakita, Y. Yoshikuni, Y. Itaya, and H. Asahi, "Monolithic integration of a DFB laser and an MQW optical modulator in the 1.5-μm wavelength range," *IEEE J. Quantum Electron.*, vol. 27, pp. 915-918, 1991.

[12] M. Suzuki, H. Tanaka, H. Taga, S. Yamamoto, and Y. Matsushima, "$\lambda/4$-shifted DFB laser/electroabsorption modulator integrated light source for multigigabit transmission," *J. Lightwave Technol.*, vol. 10, pp. 90-94, 1992.

[13] H. Soda, K. Sato, H. Sudo, S. Takeuchi, and H. Ishikawa, "Ultra-low chirp characteristics of monolithic electroabsorption modulator/DFB laser light source," in *Tech. Dig. ECOC '91*, Paris, France, Paper WeB7-1, 1991.

[14] K. Wakita, I. Kotaka, H. Asai, M. Okamoto, Y. Kondo, and M. Naganuma, "High-speed and low-drive-voltage monolithic multiple quantum well modulator/DFB laser light source," *IEEE Photon. Technol. Lett.*, vol. 4, pp. 16-18, 1992.

[15] U. Koren, B. Glance, B. I. Miller, M. G. Young, M. Chien, T. H. Wood, L. M. Ostar, T. L. Koch, R. M. Jopson, J. D. Evankow, G. Raybon, C. A. Burrus, P. D. Magill, and K. C. Reichmann, "Widely tunable distributed Bragg reflector laser with an integrated electroabsorption modulator," in *Tech. Dig. OFC '92*, San Jose, CA, Paper WG5, 1992.

[16] T. Kato, T. Sasaki, N. Kida, K. Komatsu, and I. Mito, "Novel MQW DFB laser diode/modulator integrated light source using bandgap energy control epitaxial growth technique," in *Tech. Dig. ECOC '91*, Paris, France, Paper WeB7-2, 1991.

[17] M. Aoki, H. Sano, M. Suzuki, M. Takahashi, K. Uomi, and A. Takai, "Novel structure MQW electroabsorption-modulator/DFB-laser integrated device fabricated by selective area MOCVD growth," *Electron. Lett.*, vol. 27, pp. 2138-2140, 1991.

[18] T. Kato, T. Sasaki, K. Komatsu, and I. Mito, "DFB-LD/modulator integrated light source by bandgap energy controlled selective MOVPE," *Electron. Lett.*, vol. 28, pp. 153-154, 1992.

[19] M. Aoki, M. Takahashi, M. Suzuki, H. Sano, K. Uomi, T. Kawano, and A. Takai, "High-extinction-ratio MQW electroabsorption modulator integrated DFB laser fabricated by in-plane bandgap energy control technique," *IEEE Photon. Technol. Lett.*, vol. 4, pp. 580-582, 1992.

[20] M. Aoki, M. Suzuki, M. Takahashi, H. Sano, T. Ido, T. Kawano, and A. Taki, "High-speed (10 Gbit/s) and low-drive-voltage (1 V peak to peak) InGaAs/InGaAsP MQW electroabsorption modulator integrated DFB laser with semi-insulating buried heterostructure," *Electron. Lett.*, vol. 28, pp. 1157-1158, 1992; also "High-speed and low-drive-voltage MQW EA-modulator integrated DFB laser with semi-insulating BH structure," in *Tech. Dig. 13th IEEE Int. Semiconductor Laser Conf.*, Takamatsu, Japan, Paper H-1, 1992.

[21] T. H. Wood, J. Z. Pastalan, C. A. Burrus, Jr., B. C. Johnson, B. I. Miller, J. L. Demiguel, U. Koren, and M. G. Young, "Electric field screening by photogenerated holes in MQWs: A new mechanism for absorption saturation," *Appl. Phys. Lett.*, vol. 57, pp. 1081-1083, 1990.

[22] A. M. Fox, D. A. B. Miller, G. Livescu, J. E. Cunningham, J. E. Henry, and W. Y. Jan, "Quantum well carrier sweep out: Relation to electroabsorption and exiton saturation," *IEEE J. Quantum Electron.*, vol. 27, pp. 2281-2295, 1991.

[23] T. H. Wood, T. Y. Chang, J. Z. Pastalan, C. A. Burrus, Jr., N. J. Sauer, and B. C. Johnson, "Increased optical saturation intensities in GaInAs multiple quantum wells by the use of AlGaInAs barriers," *Electron. Lett.*, vol. 27, pp. 257-259, 1991.

[24] K. W. Goossen, L. M. F. Chirovsky, R. A. Morgan, J. E. Cunningham, and W. Y. Jan, "High-power extremely shallow quantum-well modulators," *IEEE Photon. Technol. Lett.*, vol. 3, pp. 448-450, 1991.

[25] Y. D. Galeuchet and P. Roentgen, "Selective area MOVPE of GaInAs/InP heterostructures on masked and nonplanar (100) and {111} substrates," *J. Crys. Growth*, vol. 107, pp. 147-150, 1991.

[26] J. Finders, J. Geurts, A. Kohl, M. Weyers, B. Opitz, O. Kayser, and P. Balk, "Composition of selectively grown $In_xGa_{1-x}As$ structures from locally resolved Raman spectroscopy," *J. Crys. Growth*, vol. 107, pp. 151-155, 1991.

[27] E. Colas, A. Shahar, B. D. Soole, W. J. Tomlinson, J. R. Hayes, C. Caneat, and R. Bhat, "Lateral and longitudinal patterning of semiconductor structures by crystal growth on nonplanar and dielectric-masked GaAs substrates: Application to thickness-modulated waveguide structures," *J. Crys. Growth*, vol. 107, pp. 226-230, 1991.

[28] E. Colas, C. Caneat, M. Frei, E. M. Clausen, W. E. Quinn, and M. S. Kim, "In situ definition of semiconductor structures by selective area growth and etching," *Appl. Phys. Lett.*, vol. 59, pp. 2019-2021, 1991.

[29] M. Takahashi, M. Suzuki, M. Aoki, K. Uomi, and T. Kawano, "In-plane quantum energy control of InGaAs/InGaAsP MQW structure by MOCVD selective area growth," in *Tech. Dig. IPRM '92*, Newport, RI, Paper WB3, 1992.
[30] A. R. Clawson, C. M. Hanson, and T. T. Vu, "MOVPE growth of SiO_2-masked InP structures at reduced pressures," *J. Crys. Growth*, vol. 77, pp. 334–339, 1986.
[31] O. Kayser, R. Westphalen, B. Opitz, and P. Balk, "Control of selective area growth of InP," *J. Crys. Growth*, vol. 112, pp. 111–122, 1991.
[32] M. Suzuki, Y. Noda, Y. Kushiro, and S. Akiba, "Dynamic spectral width of an InGaAsP/InP electroabsorption light modulator under high-frequency large-signal modulation," *Electron. Lett.*, vol. 22, pp. 312–313, 1986.
[33] H. Kakibayashi and F. Nagata, "Composition dependence of equal thickness fringes in an electron microscope image of $GaAs/Al_xGa_{1-x}As$ multilayer structure," *Jpn. J. Appl. Phys.*, vol. 24, pp. L905–L907, 1985.
[34] T. Sasaki, Y. Sakata, N. Kida, M. Kitamura, and I. Mito, "Novel tunable DBR-LDs grown by selective MOVPE using a waveguide-direction band-gap energy control technique," in *Tech. Dig. OFC '92*, San Jose, CA, Paper FB10, 1992.
[35] T. Tanbun-Ek, P. A. Andrekson, R. A. Logan, S. N. G. Chu, D. L. Coblentz, A. M. Sergent, and K. W. Wecht, "DFB lasers with monolithically integrated passive waveguide," *IEEE Photon. Technol. Lett.*, vol. 4, pp. 685–688, 1992.
[36] M. Suzuki, M. Takahashi, M. Aoki, and T. Kawano, "Flatness of layer thickness grown by selective area MOCVD," in *Tech. Dig. 11th Record of Alloy Semicon. Phys. and Electron. Symp.*, Kyoto, Japan, Paper IV-4, 1992.

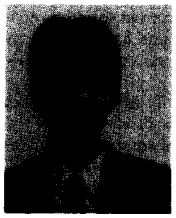

Masahiro Aoki was born in Tokyo, Japan, in 1964. He received the B.S. and M.S. degrees in physical electronics, both from the Tokyo Institute of Technology, Tokyo, Japan, in 1987 and 1989, respectively.

In 1989, he joined the Central Research Laboratory, Hitachi Ltd., Tokyo, Japan, where he has been engaged in the design and fabrication of high-speed optical devices for lightwave communications, including high-speed laser diodes and optical modulators and their monolithic integration.

Mr. Aoki is a member of the Japan Society of Applied Physics and the Institute of Electronics, Information and Communication Engineers of Japan.

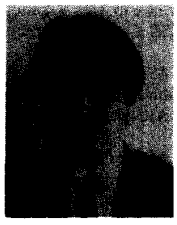

Makoto Suzuki was born in Iwate, Japan, on April 3, 1965. He graduated from the Hitachi Keihin Institute of Technology in 1987.

In 1984, he joined the Central Research Laboratory, Hitachi Ltd., Tokyo, Japan, where he has been engaged in the crystal growth of III-V compounds by MOCVD for semiconductor lasers.

Mr. Suzuki is a member of the Japan Society of Applied Physics.

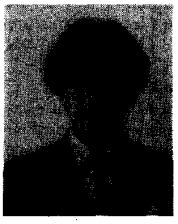

Hirohisa Sano was born in Tokushima, Japan, in 1961. He received the B.S. and M.S. degrees in communication engineering, both from Osaka University, Osaka, Japan, in 1983 and 1985, respectively.

In 1985, he joined the Central Research Laboratory, Hitachi Ltd., Tokyo, Japan, where he has been engaged in the design and fabrication of waveguide devices for lightwave communications, including optical multi/demultiplexer and high-speed optical modulators and their monolithic integration.

Mr. Sano is a member of the Japan Society of Applied Physics and the Institute of Electronics, Information and Communication Engineering of Japan.

Toshihiro Kawano was born in Kagoshima, Japan, in 1952. In 1971, he joined the Central Research Laboratory, Hitachi Ltd., Tokyo, Japan. He graduated from the Hitachi Ibaraki Institute of Technology in 1974. From 1974 to 1975, he studied as a Visiting Scholar at Tokyo Institute of Technology, Tokyo. Since then, he has been researching crystal growth (LPE and MOCVD).

Mr. Kawano is a member of the Japan Society of Applied Physics.

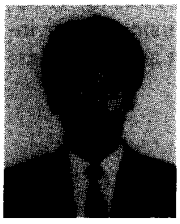

Tatemi Ido was born in Gifu, Japan, in 1967. He received the B.S. and M.S. degrees in applied physics from the University of Tokyo, Japan.

In 1991, he joined the Central Research Laboratory, Hitachi Ltd., Tokyo, Japan, where he has been engaged in the study of high-speed optical modulators.

Mr. Ido is a member of the Japan Society of Applied Physics and the Physical Society of Japan.

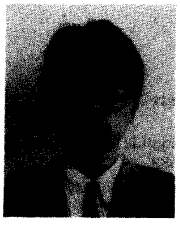

Tsuyoshi Taniwatari was born in Nagasaki, Japan, in 1969. He graduated from the Hitachi Keihin Institute of Technology, Yokohama, Japan, in 1990.

In 1987, he joined the Central Research Laboratory, Hitachi Ltd., Tokyo, Japan, where he has been engaged in the crystal growth of III-V compounds by MOCVD for semiconductor lasers.

Mr. Taniwatari is a member of the Japan Society of Applied Physics.

Kazuhisa Uomi was born in Tokushima, Japan, on November 17, 1958. He received the B.E., M.E., and Ph.D. degrees in electronics engineering from Hiroshima University, Hiroshima, Japan, in 1981, 1983, and 1990, respectively. His dissertation research included the study of ultra-high-speed semiconductor lasers, especially the proposal and investigation of modulation-doped MQW lasers.

In 1983, he joined the Central Research Laboratory, Hitachi Ltd., Tokyo, Japan, where he has been involved in research and development of semiconductor lasers, especially MQW lasers, modulation-doped MQW lasers, high-speed 1.55-μm DFB-MQW lasers, and nonlinear damping phenomena. From 1992 to 1993, he was with Bell Communications Research, Red Bank, NJ, as a visiting scientist, where he was engaged in research and InGaAsP vertical-cavity surface-emitting lasers.

Dr. Uomi has authored and coauthored over 45 papers in leading technical journals and 25 international conference papers. He is a member of the Japan Society of Applied Physics and the Institute of Electronics, Information and Communication Engineering (IEICE) of Japan. He received the Scientific Encouragement Award from IEICE in 1989, the Best Paper Award at the Optoelectronics Conference in 1990, and the Excellent Paper Award from the Japan Society of Applied Physics in 1991.